HIGH EFFICIENCY KINETIC-ALFVEN-WAVE CURRENT DRIVE

S. Puri and R. Wilhelm
Max-Planck Institut für Plasmaphysik, EURATOM Association,
Garching bei München, Federal Republic of Germany

Non-inductive current drive for attaining steady-state operation is a significant feature of the future Tokamak devices such as NET and ITER. However, the poor current-drive efficiency ($\gamma = Rn_{20}I/P \lesssim 0.4$) of the schemes presently under consideration limits the fusion power gain to $P_{fusion}/P_{auziliary} \sim 5$, which is an order of magnitude lower than the requirements of an economic fusion reactor [1].

In this paper we show that the combination of bootstrap current [2] and optimized antenna parameters can lead to high efficiency kinetic-Alfven-wave current drive in reactor-grade plasmas *with elongated cross sections*. The optimal parameters include (i) finite, non-zero azimuthal wave number $m = 1$, (ii) large toroidal wave number $n = 5 - 8$, (iii) an antenna array consisting of at least n elements with adjacent elements phased $\pi/2$ apart, (iv) Faraday shielding, and (v) plasma cross-section elongation $\varepsilon > 1.5$, which together with the finite β, helps in moderating the trapped-particle effects by locating the resonance close to the plasma axis.

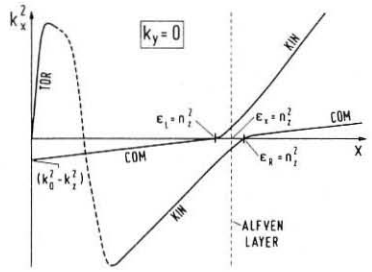

Fig. 1

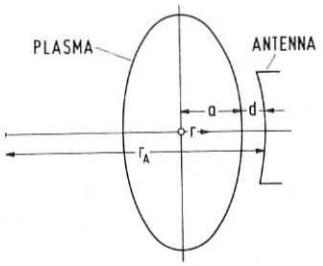

Fig. 2

Figure 1 shows the qualitative Alfven-wave dispersion characteristics in a slab geometry for $k_y = 0$. The plasma density and temperature are assumed to increase along x and the magnetic field is in the z direction. ϵ_x, ϵ_y and ϵ_z are the components of the dielectric tensor ϵ, $\mathbf{n} = \mathbf{k}/k_0$, and $\epsilon_{L,R} = \epsilon_x \pm i\epsilon_y$. The propagating cold-plasma torsional Alfven wave (TOR) becomes the evanescent hot-plasma KIN at $\zeta = v_p/v_t \approx 1$ which typically occurs close to the plasma edge for $T_e \sim 100\,eV$. Near the Alfven layer at $\epsilon_x = n_z^2$, KIN assumes a propagating character and is subject to strong Landau damping. The Alfven resonance $\epsilon_x = n_z^2$ is approached via coupling to the weakly

evanescent compressional Alfven wave (COM). Near the Alfven layer, the evanescent COM launched by the antenna partly couples to the propagating COM in the plasma interior and partly converts to the propagating KIN via the process of wave conversion [3]. The energy coupled to KIN is readily assimilated through electron Landau damping giving rise to plasma heating and current drive [3,4].

The success of this scheme is critically dependent upon two factors, namely, (i) the launching of COM with a minimum of evanescence between the antenna and the Alfven layer, and (ii) efficient wave conversion from COM to KIN near the Alfven layer. These happen to be contradictory requirements: The first is best satisfied at low values of m and n, while the second demands the choice of finite $m = 1$, and large $n = 5 - 8$ values [5,6].

The requirement of a finite azimuthal wave number $m = 1$ and a large toroidal wave number $n = 5 - 8$ imposes the serious penalty of limited radial access of the antenna energy into the plasma due to the increased evanescence experienced by COM. Acceptable antenna coupling ($Q \sim 15$) is feasible only for the resonance layer location $r_0 > 0.67a$, corresponding to a penetration depth $p = 0.33a + d$, where a is the plasma radius and d is the antenna-plasma separation [5,6]. Current drive confined to the outer one-third plasma radius would be undesirable. The present trend towards elongated plasma cross-sections together with the shift in the plasma axis due to finite β effects in reactor-grade plasmas radically improves this dismal outlook.

For the elliptical plasma cross-section of elongation ε (Fig.2), the antenna radius is given by

$$r_A \approx (a + d)\varepsilon^2 \ . \tag{1}$$

The increase in the antenna radius leads to a reduction in the wave evanescene. Since the penetration depth p is considerably less than the antenna radius, a reasonable estimate of p is possible using the slab approximation corrected for the cylindrical geometry. Let $k_y = \tilde{r}^{-1}$ and $k_z = n(R + r)^{-1}$, where $\tilde{r} = r_A - (a + d) + r$ and R is the plasma major radius. The wave evanescence causes a steady decrease of the wave amplitude as we move away from the antenna. The energy density at the resonance position r_0, relative to its value at the antenna surface is $G = \exp(-\Gamma)$, where

$$\Gamma = 2ia \int_{\rho_0}^{1+\rho_d} k_x(\rho)\, d\rho \ , \tag{2}$$

$\rho = r/a$, $\rho_0 = r_0/a$, $\rho_d = d/a$, k_x is given by the approximate COM dispersion relation

$$k_x^2 = k_0^2 \epsilon_x - k_y^2 - k_z^2 \ , \tag{3}$$

and $\epsilon_x = 1 + (n_z^2 - 1)(1 - \rho^2)/(1 - \rho_0^2)$ for a parabolic density profile. G is plotted as a function of ρ_0 and ε for $n = 6$ in Fig.3, assuming $A = R/a = 4$, $\rho_d = 0.1$, and $n_z^2 \gg 1$.

As ϵ increases from 1 to 2, ρ_0 can be lowered from 0.67 to 0.37 keeping the antenna coupling unchanged.

Further enhancement in the penetration of antenna energy into the plasma interior is contributed by the finite β in reactor-grade plasmas. Finite β is accompanied by an outward shift of the plasma axis which for the reactor parameters may amount to as much as a quarter of the plasma radius. Thus, it would be possible to locate the resonant layer at $\rho_0 \gtrsim 0.12$, i.e., practically the entire plasma volume is accessible for the KIN current drive.

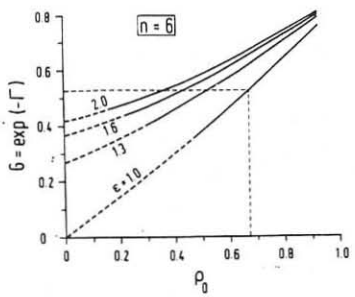

Fig. 3

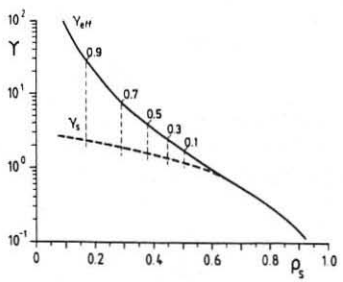

Fig. 4

The current density induced in the plasma is related to the power density by

$$j(\rho) \approx \frac{e}{m} \frac{\sigma(Z)\Omega(\rho, A)P(\rho)}{\nu_{ei}(\rho)v_A(\rho)} , \tag{4}$$

where $v_A(\rho)$ is the local Alfven speed, $\nu_{ei}(\rho)$ is the Spitzer collision frequency, $\sigma = (1 + \nu_{ei}/\nu_{ee})^{-1} = (1 + 0.5Z)^{-1}$ is the fraction of the subthermal wave momentum transferred to the bulk-plasma electrons, while $\Omega = \left[1 - (\rho/A)^{1/2}\right]^2$ is the efficacy of ohmic current drive [7] available from the momentum contained in the bulk-plasma electrons. Physically the two-step process consists of storing canonical angular momentum in the trapped particles by Ware [8] pinch and subsequent release via inverse Ware pinch, with the fraction $\sigma\Omega$ of the canonical angular momentum delivered by the wave supplying the current drive. In so far as the bootstrap current too originates from the release of stored canonical angular momentum, only the fraction $(\sigma\Omega/B_\theta)(\rho/A)^{1/2}Tdn/dr$ may be available as the net plasma current. The current-drive efficiency becomes

$$\gamma = \frac{< n_{20} > RI}{P_P} = \frac{< n_{20} >}{2\pi} \frac{e}{m} \frac{\sigma(Z) \int_0^1 j(\rho)\rho \, d\rho}{\int_0^1 \Omega^{-1}(\rho, A)\nu_{ei}(\rho)v_A(\rho)j(\rho)\rho \, d\rho} , \tag{5}$$

where $< n_{20} > \times 10^{20} m^{-3}$ is the volume-averaged plasma density. Equation (5) does not include the contribution of the bootstrap current [2] I_b to the total plasma current I_p. In the presence of the bootstrap current, the demands on the current drive in the unfavorable outer region are significantly diminished. Maximum current-drive efficiency would be obtained if the wave driven seed current $I_s = I_p - I_b$ is spread with a constant density j_s in the region $0 \leq \rho \leq \rho_s \approx \sqrt{I_s/q_a I_p}$, where q_a is the safety factor at the plasma boundary and $j_s = (2/\mu_0 r_T) B_t$ is the highest current density consistent with the MHD stability requirement $q \geq 1$. Assuming $n_e(\rho) = n_{e0}(1-\rho^2)^{\chi_n}$ and $T_e(\rho) = T_{e0}(1-\rho^2)^{\chi_T}$ yields the seed-current-drive efficiency

$$\gamma_s = \frac{13.5\mu^{1/2}\sigma(Z) < \beta >^{1/2} < T_{keV} >}{Z < \ln\Lambda >} \frac{\chi_T + 1}{\chi_n + 1} (\chi_n + \chi_T + 1)^{1/2} \Im \,, \tag{6}$$

where μ is the atomic mass number, $< \beta >$ is the volume-averaged toroidal β, $< T_{keV} >$ is the volume-averaged electron temperature in keV, and $< \ln\Lambda >$ is the weighted Coulomb logarithm. The profile and trapped-particle effects are contained in

$$\Im(\rho_s, \alpha, A) = \frac{\int_0^{\rho_s} \rho \, d\rho}{\int_0^{\rho_s} (1-\rho^2)^{-\alpha} \left[1 - (\rho/A)^{1/2}\right]^{-2} \rho \, d\rho} \,, \tag{7}$$

where, $\alpha = 1.5\chi_T - 0.5\chi_n$. The pertinent figure of merit is contained in the effective current-drive efficiency

$$\gamma_{eff} = \frac{I_p}{I_s} \gamma_s \,. \tag{8}$$

Figure 4 is a plot of γ_s and γ_{eff} as a function of ρ_s and α for $A = 4$, $\chi_n = 1$, $\chi_T = 1.5$, $\mu = 2.5$, $< \beta >= 0.05$, $< T_{keV} >= 15$, $Z = 1.5$, $q_a = 3.5$ and $< \ln\Lambda >= 17$. For $0.10 \leq I_b/I_p \leq 0.90$ (indicated along the γ curves in Fig.4), $0.50 \geq \rho_s \geq 0.17$, and $1.75 \leq \gamma_{eff} \leq 27.0$. Although the uncertainty in I_b/I_p precludes a more precise estimate of γ_{eff}, kinetic-Alfven-wave current drive promises to be a highly credible proposition and merits careful consideration.

[1]. WILHELM, R., in *Proc. 15th Symp. on Fusion Tech.*, Utrecht, 1988.
[2]. BICKERTON, R. J., Comments Plasma Phys. Controlled Fusion **1**(1972)95.
[3]. HASEGAWA, A., CHEN, L., Phys. Rev. Lett. **32**(1974)454.
[4]. HASEGAWA, A., Nuclear Fusion **20**(1980)1158.
[5]. PURI. S., Nucl. Fusion **27**(1987)229.
[6]. PURI, S., Nucl. Fusion **27**(1987)1091.
[7]. WESSON, J., in *Tokamaks*, Clarendon Press, Oxford (1987), p.95.
[8]. WARE, A. A., Phys. Rev. Lett. **25**(1970)15.